



Effect of the Revisit Interval on the Accuracy of Remote Sensing-based Estimates of Evapotranspiration at Field Scales

5 Joseph G. Alfieri¹, Martha C. Anderson¹, William P. Kustas¹, Carmelo Cammalleri²

¹US Department of Agriculture, Agricultural Research Service,
Hydrology and Remote Sensing Laboratory, Beltsville, MD, USA

²Joint Research Centre, European Commission, Ispra, Italy

Correspondence to: Joseph G. Alfieri (joe.alfieri@ars.usda.gov)



Abstract. Accurate spatially distributed estimates of actual evapotranspiration (ET) derived from remotely sensed data are critical to a broad range of practical and operational applications. However, due to lengthy return intervals and cloud cover, data acquisition is not continuous over time, particularly for satellite sensors operating at medium (~100 m) or finer resolutions. To fill the data gaps between clear-sky data acquisitions, interpolation methods that take advantage of the relationship between ET and other environmental properties that can be continuously monitored are often used. This study sought to evaluate the accuracy of this approach, which is commonly referred to as temporal upscaling, as a function of satellite revisit interval. Using data collected at 20 Ameriflux sites distributed throughout the contiguous United States and representing 4 distinct land cover types (cropland, grassland, forest, and open canopy) as a proxy for perfect retrievals on satellite overpass dates, this study assesses daily ET estimates derived using 5 different reference quantities (incident solar radiation, net radiation, available energy, reference ET, and equilibrium latent heat flux) and 3 different interpolation methods (linear, cubic spline, and hermite spline). Not only did the analyses find that the temporal autocorrelation, i.e. persistence, of all of the reference quantities was short, it also found that those land cover types with the greatest ET exhibited the least persistence. This carries over to the error associated with both the various scaled quantities and flux estimates. In terms of both the root mean square error (RMSE) and mean absolute error (MAE), the errors increased rapidly with increasing return interval following a logarithmic relationship. Again, those land cover types with the greatest ET showed the largest errors. Moreover, using a threshold of 20% relative error, this study indicates that a return interval of no more than 5 days is necessary for accurate daily ET estimates. It also found that the spline interpolation methods performed erratically for long return intervals and should be avoided.



1 Introduction

Because it is a fundamental linkage between numerous biogeophysical and biogeochemical processes, accurate information regarding evapotranspiration (ET) is critical for a broad range of scientific and practical applications with significant social, economic, and environmental impacts. For example, reliable information about ET is essential for accurately forecasting weather and assessing the impacts of changing climate (Katul et al., 2012; Wang and Dickinson, 2012); monitoring and mitigating the adverse effects of extreme weather events such as drought (Anderson et al., 2007, 2011, 2016; Otkin et al. 2016); and, identifying and predicting the changes in both the biogeographical characteristics of ecosystems and the services they provide in response to changing environmental conditions (Hawkins and Porter, 2003; Kreft and Jetz, 2007; Midgley et al. 2002). However, as pointed out by Seguin and Itier (1983), Abdelghabi et al. (2008), and Anderson et al. (2012), among others, perhaps the most important application of ET data is providing information critical to satisfying the competing demands for scarce water resources.

Already, the competing demands for fresh water by agricultural, industrial, and urban consumers exceed the available supply for nearly one-third of the world's population (Qadir et al. 2003) and it is predicted that number will increase to more than two-thirds of the global population in the coming decades (Wallace, 2008; Vörösmarty et al., 2010). To meet the current and future demand for water, resource managers and other policymakers must make informed decisions regarding the needs of competing stakeholders when allocating limited water resources in order to maximize their effective use. In the case of irrigated agriculture, which is the largest consumer of fresh water and accounts for 1200 km³ or approximately 85% of annual current water use (Drooger et al., 2010; Thenkabail et al., 2010), the need for water is largely driven by evaporative loss. Thus, ET data are needed not only to monitor evaporative water loss in order to determine crop irrigation needs, it is also needed to develop the irrigation techniques and management practices necessary to ensure the efficient use of water in agricultural environments (Howell, 2001; Schultz and Wrachien, 2002; Gordon et al., 2010; de Fraiture and Wichelns, 2010).

While in situ observations are invaluable for some of these applications, many of them require spatially distributed measures of ET at field to continental scales that cannot be supplied by existing flux measurement infrastructure. Remote sensing-based approaches are the only viable mean for monitoring ET over this continuum of scales (McCabe et al., 2008; Kalma et al., 2008; Gonzalez-Dugo et al., 2009). As discussed by Anderson et al. (2012), any comprehensive program for monitoring water resources will by necessity use remote sensing data collected by multiple platforms at a range of spatial and temporal scales.

Nonetheless, remote sensing is not without limitations. Chief among these is the infrequent acquisition of the medium to high-resolution imagery needed to determine ET via remote sensing-based models either because of a lengthy return interval or the presence cloud cover (Ryu et al., 2012; van Niel et al., 2012; Cammalleri et al., 2013). To provide temporally continuous ET estimates between overpasses, the moisture flux for the periods between data acquisitions is often estimated using an interpolation technique commonly referred to temporal upscaling. This well-established approach, which



can be applied at either sub-daily or daily time steps, estimates the moisture flux as the product of some reference quantity (χ) and its associate scaled metric (f) according to:

$$\widehat{ET}_t = \chi_t f_t \quad (1)$$

where \widehat{ET} is the estimated ET and t indicates the time period of the estimate. While it is typically related to the moisture flux, χ is a quantity that can be measured or estimated more readily than the moisture flux itself. The scaled metric is the ratio between χ and the moisture flux. For example, it is quite common to estimate ET expressed in terms of the latent heat flux (λE) using the available energy (A) as the reference quantity and evaporative fraction (f_A) as the scaled metric (e.g. Crago and Brutsaert, 1996; Bastiaanssen et al., 1998; Suleiman and Crago, 2004; Colaizzi et al., 2006; Hoedjes et al. 2008; van Niel et al., 2011; Delogu et al., 2012).

For the periods between data retrievals, f is estimated via interpolation. As a result, this approach is predicated on the assumption that f is self-preserving, i.e. it is constant or nearly constant, varying only slowly over time (Brutsaert and Sugita, 1992; Nichols and Cuenca, 1993; Crago, 1996). In order to conform to this assumption, the components of the radiation or energy budget are often selected as χ such that f is an analogue of evaporative fraction. Examples of these quantities include the incident solar radiation ($K\downarrow$; Jackson et al. 1983; Zhang and Lemeur, 1995), or extraterrestrial solar radiation ($K\downarrow_{TOA}$; Ryu et al. 2012). However, a number of recent studies indicate the assumption of self-preservation is only approximate for these quantities. For example, both Gentine et al. (2007) and Hoedjes et al. (2008) showed that the self-preservation of evaporative fraction is sensitive to soil moisture conditions and fractional vegetation cover. Similarly, Van Niel et al. (2012) showed that the degree of self-preservation can be influenced by cloud cover and pointed out that assuming clear-sky conditions could result in significant errors in the moisture flux estimates.

Moreover, since cloud cover can hamper self-preservation, temporal upscaling is also underpinned by the implicit assumption of clear-sky conditions. However, because the validity of this assumption is dubious even over the course of a single day, it is rarely enforced (Van Niel et al., 2012) As such, the assumption of clear-sky conditions is a significant potential source of error in the ET estimates that must be considered when utilizing or evaluating temporally upscaled moisture flux data (van Niel et al., 2012; Peng et al., 2013; Cammalleri et al., 2014).

Other studies have focused on using a quantity derived from the local meteorological conditions as χ because it would consider many of the meteorological factors that influence the moisture flux. For example, and Tasumi et al. (2005) proposed using the reference ET for alfalfa (ET_r) as χ ; later, Allen et al. (2007) proposed using the standardized reference evapotranspiration (ET_0) as χ . In both cases, the resulting f is equivalent to a crop coefficient and would share its characteristics. As a result, f derived from ET_r or ET_0 can be treated in much the same fashion as a crop coefficient and assumed to be nearly constant changing only slowly with time. (Colaizzi et al., 2006; Chavez et al., 2009).

The aim of this study is to assess the error introduced into ET estimates by temporal upscaling under realistic conditions. Specifically, this study uses in situ measurements collected over a variety of land cover types as a proxy for remotely-sensed data to evaluate the impact of multiple reference quantities, interpolation techniques, and revisit intervals on the estimated daily moisture flux. The study focuses on daytime mean data to evaluate temporal upscaling at a daily time



step. It also assumes perfect retrieval of the flux; in other terms, no error is introduced into ET data to approximate error or uncertainty in the estimates of ET from remote sensing-based models. By doing so, this study seeks to provide insights into the relative strengths of the differing temporal upscaling approaches and to discern a maximum return interval threshold for obtaining acceptable estimates of daily ET. The following section provides an overview of the field measurements along with the reference quantities, interpolation techniques, and evaluation methods used in this study. Section 3 provides a discussion of the results of this study while the final section encapsulates the conclusions that can be drawn from those results.

2. Methods

2.1. Datasets

Data, including local meteorological conditions, surface fluxes, and surface conditions (Table 1), collected at numerous sites within the Ameriflux network (Baldocchi et al., 2001) were used for this study. Specifically, the data were collected at 20 Ameriflux sites (Table 2) distributed across the contiguous United States and represent four distinct land cover types. Namely, these are *i.* croplands (maize/soy rotation); *ii.* grasslands; *iii.* forests (evergreen needleleaf and broadleaf deciduous); and, *iv.* open-canopy (shrubland and woody savanna). Measurements were collected for a minimum of five years at each of the sites selected. Further information regarding the field sites, measurement procedures, and post-processing protocols for Ameriflux is presented in Baldocchi et al., 2001; the data are archived at the Oak Ridge National laboratory and available at <http://ameriflux.ornl.gov/>.

After forcing closure of the energy balance while by maintaining a constant Bowen ratio (Twine et al. 2000) in order to more closely match the characteristics of the output from energy balance models, the 30-minute measurements were used to calculate the various χ and f . Next, the daytime mean of these quantities and the fluxes were calculated for use in the subsequent analyses. Although it can be taken as nominally as the period between 0800 and 1800 LST, daytime is defined herein as the period between the first and last measurements during a given day when the incident solar radiation exceeded 100 W m^{-2} .

2.2. Reference Quantities and Scaled Metrics

For this study, five χ , along with their associated f , discussed in the literature were evaluated. The first three of these quantities ($K\downarrow$, R_n , and A) yield analogues of evaporative fraction and require incrementally greater information regarding the surface radiation and energy budgets. (Hereafter, the associated scaled metrics are denoted as f_χ where the subscript represents the reference quantity; for example, the ratio of λE and A is indicated as f_A .) The remaining χ are derived from estimates of the moisture flux calculated based on local meteorological conditions. These are ET_0 expressed in terms of energy (λE_0) and the equilibrium latent heat flux (λE_{eq}). The first of these, λE_0 , is described by Allen et al. (1998) as the hypothetical ET (or λE) from a grass reference surface with an assumed height of 0.12 m, albedo of 0.23, and surface



resistance of 70 s m^{-1} which would be typical of a moderately moist soil. It is defined using a simplified form of the Penman-Monteith relationship as:

$$\lambda E_0 = \lambda_v \frac{a\Delta A + \gamma \frac{C_n U D}{T_K}}{\Delta + \gamma(1 + U C_d)} \quad (2)$$

where λ_v is the latent heat of vaporization (J kg^{-1}), a is a constant ($1.1333 \times 10^{-4} \text{ kg J}^{-1}$), Δ is the slope of the saturation vapor pressure-temperature curve (kPa K^{-1}), A is the available energy (W m^{-2}), γ is the psychrometric constant (kPa K^{-1}), C_n is a constant ($1.1333 \times 10^{-5} \text{ K s}^2 \text{ m}^{-2}$), T_K is the air temperature (K), U is the wind speed (m s^{-1}), D is the water vapor pressure deficit (kPa), and C_d is a constant (0.25 s m^{-1} ; Allen et al., 1998). Similarly, λE_{eq} , which can be thought of as the energy-driven moisture flux that is independent of surface resistance, can be expressed according to:

$$\lambda E_{eq} = A \frac{\Delta}{\Delta + \gamma} \quad (3)$$

with the variables defined as above (McNaughton, 1976; Raupach, 2001).

2.3. Interpolation Techniques

In addition to piecewise linear interpolation, two piecewise spline interpolation methods were evaluated as a part of this study, namely cubic and hermite spline interpolation. (These are indicated when necessary hereafter by the subscripts L, S, H, respectively.) In contrast to linear interpolation, which tends to yield accurate results only when the underlying data vary smoothly over time, the splining methods are less prone to error when the observed data change abruptly (Trefethen 2013). Similarly, the more computational complex hermite spline method typically yields more accurate results when the gaps between observed data points are large (DeBoor, 1994).

For this analysis, the temporal upscaling was conducted using daytime mean data and all possible combinations of f and interpolation methods at each Ameriflux site. Moreover, in order to maximize the robustness of the statistical analysis, all possible realizations were evaluated. Each realization is one of the unique yet equivalent subsets that can be generated from the data collected at a particular site while maintaining constant return interval. The total number of possible realizations for a given return interval is equal to the length in days of the return interval. The individual realizations were generated by performing the analysis beginning on consecutive days. For example, in the case of a three-day return interval, three unique realizations can be generated. The first contains the data points for day of year 1, 4, 7, ... 364; the second contains the data points for day of year 2, 5, 8, ... 365; and, the third contains the data points for day of year 3, 6, 9, ... 363.

Again, to emulate the temporal upscaling of flux data derived from remotely sensed-data as closely as possible, efforts were made to ensure that the observations used for the interpolation were collected on clear-sky days. Clear-sky days were identified as those where the daytime mean of the measured $K\downarrow$ was within 25% of the predicted value from a simple radiation model. The incident solar radiation was estimated as the product of $K\downarrow_{\text{TOA}}$ calculated following Meeus et al. (1991) and atmospheric transmissivity calculated according to Brutsaert (1975). In order to ensure a constant return interval for a



given interpolation, if a day was judged to be cloudy, both the observed flux on that day and the estimated flux for those subsequent days derived from it were omitted from the statistical analysis.

2.4. Statistical Metrics

As discussed by Wilks (2006), persistence, *i.e.* the degree of self-preservation, can be assessed via auto-correlation (ρ). For a given lag (h), *i.e.* the offset between measurements pairs, the auto-correlation is defined according to:

$$\rho = \frac{\sum_{i=1}^{n-h} (x_i - \bar{x}_-)(x_{i+h} - \bar{x}_+)}{\sqrt{\sum_{i=1}^{n-h} (x_i - \bar{x}_-)^2 \sum_{i=1}^{n-h} (x_{i+h} - \bar{x}_+)^2}} \quad (4)$$

where n is the number of data points, \bar{x}_- is the mean of the first $n - h$ data points and \bar{x}_+ is the mean of the final $n - h$ data points.

Three statistics are used to evaluate the accuracy of the temporal upscaling. The first of these is the root mean square error (RMSE):

$$\text{RMSE} = \sqrt{\frac{1}{n} \sum_{i=1}^n (x_i - \hat{x}_i)^2} \quad (5)$$

where n is the number of data points, x is the observed flux, and \hat{x} is the flux predicted by temporal upscaling. However, because the squared difference term in RMSE tends to overemphasize the effects of large errors (Legates and McCabe, 1999; Willmott and Matsuura, 2005; Willmott et al., 2012), the mean absolute error (MAE) was also calculated as follows:

$$\text{MAE} = \frac{1}{n} \sum_{i=1}^n |x_i - \hat{x}_i| \quad (6)$$

with the variables defined as above. The third metric is the modified index of agreement (D) defined by Willmott et al. (1985) as:

$$D = 1 - \frac{\sum_{i=1}^n |x_i - \hat{x}_i|}{\sum_{i=1}^n |x_i - \bar{x}| + |\hat{x}_i - \bar{x}|} \quad (7)$$

where \bar{x} is the mean of the observational data and the other variables are defined as above. Like MAE, the use of the absolute difference for this metric circumvents the tendency of similar statistics based on squared errors to be overly influenced by outliers or large errors.

Once calculated for individual the sites, the statistics were aggregated to represent the typical results for a given land cover type. The aggregation was accomplished by calculating the arithmetic means after conducting any necessary transform. For example, the auto-correlation was aggregated by averaging the results for the individual analysis periods and sites after applying a Fisher z transformation (Burt and Barber, 1996). Similarly, the RMSE data was averaged after first transforming it to the mean square error.



3. Results and Discussion

3.1 Persistence of Scaled Quantities

Due to its importance in determining the accuracy of the estimates, the persistence or degree of self-preservation exhibited by the various f used in this study was evaluated by determining its autocorrelation function. For each site, the autocorrelation was calculated for each contiguous segment of daytime mean data that was at least 48 days in length (1.5 times the maximum return interval considered herein).

As can be seen in Fig. 1, which shows the mean auto-correlation function for each f and land cover type, all f performed similarly. In all cases, ρ decreased in inverse proportion to h , dropping to less than 0.50 within three to ten days. Also, for any given land cover, the mean auto-correlation functions for the analogues of evaporative fraction, namely f_{K1} , f_{Rn} , and f_A , were statistically indistinguishable from one another based on t-tests conducted at the 95% confidence level. Similarly, no statistically significant difference between the mean auto-correlation functions of $f_{\lambda EO}$ and $f_{\lambda Eeq}$ was found. Nonetheless, there were statistically significant, albeit modest, differences between the auto-correlation functions associated with f derived from evaporative fraction analogues and those derived meteorological data. Regardless of land cover, ρ associated f_{K1} , f_{Rn} , and f_A , tended to be greater than ρ associated with either $f_{\lambda EO}$ or $f_{\lambda Eeq}$. On average, the difference was approximately 0.03.

The results of this analysis, which are consistent with results of other studies (Farah et al. 2004; Lu et al., 2013) that found significant day-to-day and seasonal variations in evaporative fraction, indicates the long-term persistence of f is very limited. This result also suggests that interpolated values of f may not accurately reflect the actual values and, as a result, may be a key source of error when using temporal upscaling to estimate the moisture flux between image retrievals.

Further analysis shows differences in the mean autocorrelation functions exist between land cover types. Regardless of the scaled quantity considered, the mean autocorrelation function decreases most rapidly over forested sites and the most slowly over the open canopy sites. Indeed, if the lag where the mean autocorrelation function reaches some threshold value, e.g. 0.50, is plotted as a function of the mean daytime latent heat flux (Fig. 2), it can be seen that persistence decreases exponentially with the increasing moisture flux. This suggests the return interval necessary to achieve accurate estimates of ET via temporal upscaling will be longer over relatively dry regions with a low moisture flux than over regions where ET is high.

3.2 Accuracy of the Interpolated Scaled Quantities

Both RMSE and MAE of the interpolated estimates of each χ were calculated for all land cover types and return intervals up to 32 days. As can be seen in Fig. 3 and Fig. 4, both metrics behaved similarly; regardless of the land cover type, scaled quantity, or interpolation method considered, the error increased rapidly with increasing return interval until a plateau was reached. In all cases, the RMSE, which increased according to a logarithmic function of return interval, reached 75% of its peak value within five days. Although it also increased logarithmically, the amount of time needed for MAE to reach 75%



of the peak value was more variable, ranging between 5 to 10 days. Further, MAE increased most rapidly for those land cover types that exhibited the highest moisture flux. The largest error, whether measured in terms of RMSE or MAE, also tended to be associated with the forest and cropland sites where the mean ET was largest.

The results also show that all of the interpolation methods yielded similar results for short return intervals of less than eight days. In contrast, for longer return intervals, both RMSE and MAE of the estimates using the spline interpolation methods were greater than when linear interpolation is used (Fig.3 and 4). Moreover, the error of the estimates tended to much noisier for the spline techniques, particularly the cubic spline method which exhibited periods of very large errors. These large noisy errors, which are most evident for RMSE – perhaps because it is more sensitive to outliers than MAE – are indicative of “overshoot” errors by the spline interpolation. The large errors are also most pronounced for those land cover types that also demonstrated the highest average ET and the lowest autocorrelation

3.2 Accuracy of the Latent Heat Flux Estimates

Not unexpectedly, the accuracy of the moisture fluxes estimated via temporal upscaling closely mirrors the accuracy of the interpolated f . As was the case with f , both the RMSE and MAE of the flux estimates increase rapidly with return interval to a maximum value following a logarithmic function (Fig. 5 and Fig 6.). In the case of RMSE, the maximum error ranged between 31 W m⁻² and 66 W m⁻². In the case of MAE, it ranged between 22 W m⁻² and 54 W m⁻². Again, the greatest error is associated with the land cover with the highest ET, i.e. forest and cropland.

These plots, like those for f , show little difference among the interpolation techniques when the return interval is short. For return intervals longer than about 8 days, however, the spline interpolation techniques, and especially the cubic spline method, can introduce large errors into the flux estimates due to the “overshoot” errors in the interpolation of f . These large noisy errors are most evident in the RMSE of forested sites (Fig. 5), but may also be seen to a lesser extent at the cropland sites. Overall, this suggests there is no substantive advantage of using the more computational complex spline techniques over linear regression; rather, the propensity of spline methods to introduce large errors due to interpolation “overshoot” indicates these techniques should be avoided.

The accuracy, and thus utility, of the various f was evaluated while focusing specifically on the results when linear interpolation was used. Regardless of f , based on an intercomparison of the estimated fluxes using t-tests conducted at the 95% confidence level, there was no statistically significant difference in either the flux estimates or the error due to temporal upscaling when the return interval was short, less than eight days. For longer return intervals, analyses using RMSE (Fig. 7) and MAE (not shown), which yielded similar results, indicated the error due temporal upscaling was very similar when f_{Rn} , f_A , or $f_{\lambda Eq}$ was used. Indeed, the error introduced using any of these three quantities was statistically identical based on t-tests conducted at the 95% confidence level. Moreover, with the exception of the forest sites, where the error due to temporal upscaling using $f_{K\downarrow}$ was the same as the error introduced by using f_{Rn} , f_A , or $f_{\lambda Eq}$, temporal upscaling using f_{Rn} , f_A , and $f_{\lambda Eq}$ consistently introduced the least error. For a 10-day return interval, as an example, the percent error introduced by these quantities ranges between 21% and 23% depending on land cover. In contrast, temporal upscaling using $f_{\lambda EO}$ introduced the



greatest error. Again, for a 10-day return interval, the percent error associated with $f_{\lambda EO}$ ranges between 24% and 30% depending on land cover.

The analysis of D reinforces the earlier results. Initially, D decreases rapidly with increasing return interval to less than 0.75 within 3 days and less than 0.50 within 4 to 7 days. This sharp decline in D , which is consistent for all land cover types and f (Fig. 8), indicates there is only moderate agreement between the observed flux and that estimated via temporal upscaling for all but the shortest return intervals. Also, while the moisture flux estimated using f_{Rn} tends to maintain the highest degree of agreement, followed closely by estimates using f_A , and $f_{\lambda Eq}$, the variability in D tends to be modest; for any given land cover type and return interval, D varies by 0.024, on average. These results reconfirm the earlier results by indicating that the accuracy of temporal upscaling is greatest for f_{Rn} , f_A , and $f_{\lambda Eq}$.

10 3.3 Estimating Optimal Return Interval Thresholds

Again focusing on the flux estimates when linear interpolation was used, the return interval threshold yielding errors of less than 20% in the daily ET estimates was identified (Table 3). The 20% threshold was selected because it is the nominal uncertainty commonly associated with in situ observations such as those collected via eddy covariance. While the return interval associated with the 20% threshold varied depending on land cover type and f , the longest return intervals are associated with $f_{\lambda Eq}$ followed by f_{Rn} , and f_A , which yield statistically identical results, and finally $f_{K\downarrow}$ and $f_{\lambda EO}$, which also yield statistically indistinguishable results based on t-tests at the 95% confidence level. The range of values among the various f was 2 days, on average. This again indicates that the accuracy of temporal upscaling is greatest for f_{Rn} , f_A , and $f_{\lambda Eq}$.

By plotting the average threshold return interval for each land cover class against its corresponding mean latent heat flux for that class (Fig. 9), it can be seen that length of the return interval that will result in no more than 20% error decreases with the increasing moisture flux. Like ρ , the relationship follows an exponential decay function. In this case, however, the curve has a lower bound of five days. Based on this, the maximum return interval that can be expected to introduce less than 20% error to the flux estimates via temporal upscaling for all land cover classes is 5 days. If a threshold of 10% relative error is used, the threshold falls to only 3 days.

4. Conclusions

The results of this study indicate that the day-to-day persistence of χ typically used in the temporal upscaling of satellite-based ET retrievals is quite limited. The autocorrelation of daytime means of these quantities decreases to less than 0.5 within 10 day and to less than 0.25 in 7 to 24 days depending on land cover class. More generally, it was found that the number of days for ρ to reach to a given threshold decreases with increasing λE following a well-defined exponential decay function. This suggests that the utility of temporal upscaling is limited to short return intervals, especially for land covers such as forest and croplands, which are characterized by large moisture fluxes. The analyses of RMSE and MAE confirm this inference; in both cases the magnitude of the error increases rapidly with increasing return interval and typically reaches



75% of the maximum error within 3 to 7 days. Again, the magnitude of the error due to temporal upscaling was greatest over those land cover types with the highest ET. Using 20% relative error as the threshold, the maximum return interval ranged between five and eight days, on average, depending on land cover type. However, since the maximum return interval decreases to a minimum of five days following an exponential decay function of the mean moisture flux, five days is the longest return interval that would allow for accurate ET estimates over all land cover types assuming perfect retrieval. While the study found that using λE_{eq} , R_n , or A as χ tended to produce the most accurate estimates of λE for longer return intervals, for return intervals of five days or less, there was no statistically significant difference in the flux estimates. Finally, the comparison of interpolation methods indicated there is no advantage to using the more computationally complex spline interpolation methods.

10 Acknowledgements:

The authors would also like to thank NASA for support of this research [NNH13AW37I]. They would also like to acknowledge the Ameriflux network and the investigators who contributed to the data in this study. Funding for Ameriflux is provided by the U.S. Department of Energy's Office of Science. Ameriflux data are available at <http://ameriflux.ornl.gov/>. The USDA is an equal opportunity employer.



5. References

- Abdelghani, C., Hoedjes, J. C. B., Rodriquez, J. - C., Watts, C. J., Garatuza, J., Jacob, F., and Kerr, Y. H.: Using remotely sensed data to estimate area-averaged daily surface fluxes over a semi-arid mixed agricultural land, *Agric. Forest Meteorol.*, 148: 330-342, 2008.
- 5 Allen, R. G., Pereira, L. S., Raes, D., and Smith, M.: Crop evapotranspiration, *Guideline for computing crop water requirements*, FAO irrigation and drainage paper n. 56, 326 pp., Rome, Italy, 1998.
- Allen, R. G., Tasumi, M., and Trezza, R.: Satellite-based energy balance for mapping evapotranspiration with internalized calibration (METRIC)-model, *J. Irrig. Drain. Eng.*, 133, 380-394, 2007.
- Anderson, M. C., Norman, J. M., Mecikalski, J. R., Otkin, J. A., and Kustas, W. P.: A climatological study of
10 evapotranspiration and moisture stress across the continental United States based on thermal remote sensing: 2. Surface moisture climatology, *J. Geophys. Res.*, doi:10.1029/2006JD007507, 2007.
- Anderson, M. C., Hain, C., Wardlow, B., Pimstein, A., Mecikalski, J. R., and Kustas, W.P.: Evaluation of drought indices based on thermal remote sensing of evapotranspiration over the continental United States, *J. Climate*, 15, 2025-2044, 2111.
- Anderson, M. C., Allen, R. G., Morse, A., and Kustas, W. P.: Use of Landsat thermal imagery in monitoring
15 evapotranspiration and managing water resources, *Remote Sens. Environ.*, 122, 56-65, 2012.
- Anderson, M. C., Zolin, C. A., Sentelhas, P. C., Hain, H. R., Semmens, K., Tugrul Yilmaz, M., Gao, F., Otkin J. A., Tetrault, R.: The evaporative stress index as an indicator of agricultural drought in Brazil: An assessment based on crop yield impacts, *Remote Sens. Environ.*, 174, 82-99.
- Baldocchi, D., Falge, E., Gu, L. H., Olson, R., Hollinger, D., Running, S., Anthoni, P., Bernhofer, C., Davis, K., Evans, R.,
20 Fuentes, J., Goldstein, A., Katul, G., Law, B., Lee, X., Malhi, Y., Meyers, T., Munger, W., Oechel, W., Paw, K. T., Pilegaard, K., Schmid, H. P., Valentini, R., Verma, S., Vesala, T., Wilson, K., and Wolfsy, S.: FLUXNET: A new tool to study the temporal and spatial variability of ecosystem-scale carbon dioxide, water vapor, and energy flux densities, *Bull. Amer. Meteorol. Soc.*, 82, 2415–2434, 2001.
- Bastiaanssen, W. G. M., Menenti, M., Feddes, R. A., and Holtslag, A. A. M.: A remote sensing surface energy balance
25 algorithm for land (SEBAL): 1. Formulation. *J. Hydrol.*, 212-213, 198-212, 1998.
- Brutsaert, W.: On a derivable formula for longwave radiation from clear skies. *Water Resour. Res.*, 11, 742-744, 1975.
- Brutsaert, W. and Sugita, M.: Application of self-preservation in the diurnal evolution of the surface energy budget to determine daily evaporation, *J. Geophys. Res.*, 97, 18377–18382, 1992.
- Burt, J. E., and Barber, G. M.: *Elementary statistics for Geographers*. Guilford Press, New York, New York, USA, 1996.
- 30 Cammalleri, C., Ciraolo, G., La Loggia, G., and Maltese, A.: Daily evapotranspiration assessment by means of residual surface energy balance modeling: A critical analysis under a wide range of water availability. *J. Hydrol.*, 452–453, 119–129, 2012.



- Cammalleri, C., Anderson, M. C., Gao, F., Hain, C. R., and Kustas, W.P.: A data fusion approach for mapping daily evapotranspiration at field scale, *Water Resour. Res.*, 49, 4672–4686, 2013.
- Cammalleri, C., Anderson, M.C., and Kustas, W.P.: Upscaling of evapotranspiration fluxes from instantaneous to daytime scales for thermal remote sensing applications. *Hydrol. Earth Syst. Sci.*, 18, 1885-1894, 2014.
- 5 Chavez, J. L., Neale, C. M. U., Prueger, J. H., and Kustas, W. P.: Daily evapotranspiration estimates from extrapolating instantaneous airborne remote sensing ET values, *Irrig. Sci.*, 27, 67–81, 2008.
- Colaizzi, P. D., Evett, S. R., Howell, T. A., and Tolk, J. A.: Comparison of five models to scale daily evapotranspiration from one-time-of-day measurements, *Trans. ASABE*, 49, 1409–1417, 2006.
- Crago, R.: Conservation and variability of the evaporative fraction during the daytime, *J. Hydrol.*, 180, 173–194, 1996.
- 10 Crago, R. D., and Brutsaert, W.: Daytime evaporation and the self-preservation of the evaporative fraction and the Bowen ratio, *J. Hydrol.*, 178, 241-255, 1996.
- De Boor, C.: *A Practical Guide to Splines*. Springer-Verlag, New York, New York, USA, 1994.
- de Fraiture, C., and Wichelns, D.: Satisfying future water demands for agriculture, *Agric. Water. Manag.*, 97, 502–511, 2010.
- 15 Delogu, E., Boulet, G., Olioso, A., Coudert, B., Chirouze, J., Ceschia, E., Le Dantec, V., Marloie, O., Chehbouni, G., and Lagouarde, J.-P.: Reconstruction of temporal variations of Evapotranspiration using instantaneous estimates at the time of satellite overpass, *Hydrol. Earth Syst. Sci.*, 16, 2995–3010, 2012.
- Droogers, P., Immerzeel, W. W., and Lorite, I. J.: Estimating actual irrigation application by remotely sensed evapotranspiration observations, *Agric. Water Manag.*, 97, 1351-1359, 2010.
- 20 Farah, H. O., Bastiaanssen, W. G. M., and Feddes, R. A.: Evaluation of the temporal variability of the evaporative fraction in a tropical watershed, *Int. J. Appl. Earth Obs. Geoinfo.*, 5, 129-140, 2004.
- Gentine, P., Entekhabi, D., Chehbouni, A., Boulet, G., and Duchemin, B.: Analysis of evaporative fraction diurnal behavior, *Agric. Forest Meteorol.*, 143, 13–29, 2007.
- Gonzalez-Dugo, M. P., Neale, C. M. U., Mateos, L., Kustas, W. P., Prueger, J. H., Anderson, M. C., and Li, F.: A
25 comparison of operational remote sensing-based models for estimating crop evapotranspiration, *Agric. Forest Meteorol.*, 149, 1843-1853, 2009.
- Gordon L. J., Finlayson, C., and Falkenmark M.: Managing water in agriculture for food production and other ecosystem services, *Agric. Water. Manag.*, 97: 512–519, 2010.
- Hawkins, B. A., and Porter, E. E.: Relative influences of current and historical factors on mammal and bird diversity patterns in deglaciated North America, *Global Ecol. Biogeo.*, 12, 475–481, 2003.
- 30 Hoedjes, J. C. B., Chehbouni, A., Jacob, F., Ezzahar, J., and Boulet, G.: Deriving daily evapotranspiration from remotely sensed instantaneous evaporative fraction over olive orchard in semi-arid Morocco. *J. Hydro.*, 354, 53-64.
- Howell, T. A.: Enhancing water use efficiency in irrigated agriculture, *Agron. J.*, 93: 281–289, 2001.



- Jackson, R. D., Hatfield, J. L., Reginato, R. J., Idso, S. B., and Pinter Jr., P. L.: Estimation of daily evapotranspiration from one time-of-day measurements, *Agric. Water Manage.*, 7: 351–362, 1983.
- Kalma, J. D. McVicar, T. R., and McCabe, M. D.: Estimating land surface evaporation: A review of methods using remotely sensed surface temperature data, *Surv. Geophys.*, 29: 421–469, 2008.
- 5 Katul, G. G., Oren, R., Manzano, S., Higgins, C., and Parlange, M. B.: Evapotranspiration: A process driving mass transport and energy exchange in the soil-plant-atmosphere-climate system, *Rev. Geophys.*, 50, doi:10.1029/2011RG000366, 2012.
- Kreft, H., and Jetz, W.: Global patterns and determinants of vascular plant diversity, *Proc. Nat. Acad. Sci. USA*, 104: 5925–5930, 2007.
- Legates, D. R., and McCabe, G. R.: Evaluating the use of "goodness-of-fit" measures in hydrologic and hydroclimatic model validation, *Water Resour. Res.*, 35, 233–241, 1999.
- 10 Lu, J., Tang, R., Tang, H., and Li, Z.-L.: Derivation of daily evaporative fraction based on temporal variations in surface temperature, air temperature, and net radiation, *Remote Sens.*, 5, 5369–5396, 2013.
- McCabe, M. F., Wood, E., Wojcik, R., Pan, M., Sheffield, J., Gao, H., and Su, H.: Hydrological consistency using multi-sensor remote sensing data for water and energy cycle studies, *Remote Sens. Environ.*, 112, 430–444, 2008.
- 15 McNaughton, K. G.: Evaporation and advection I: evaporation from extensive homogeneous surfaces, *Quart. J. R. Met. Soc.*, 102, 181–191, 1976.
- Meeus, J.: *Astronomical algorithms*, Willmann-Bell, Richmond, Virginia, USA, 1999.
- Midgley, G. F., Hannah, L., Millar, D., Rutherford, M. C., and Powrie, L. W.: Assessing the vulnerability of species richness to anthropogenic climate change in a biodiversity hotspot, *Global Ecol. Biogeogr.*, 11, 445–451, 2002.
- 20 Nichols, W., and Cuenca, R. H.: Evaluation of the evaporative fraction for parameterization of the surface, energy-balance, *Water Resour. Res.*, 29: 3681–3690, 1993.
- Otkin, J. A., Anderson, M. C., Hain, C., Svoboda, M., Johnson, D., Mueller, R., Tadess, T., Wardlow, B., and Brown, J.: Assessing the evolution of soil moisture and vegetation conditions during the 2012 United States flash drought, *Agric. Forest Meteorol.*, 208–219, 230–242.
- 25 Peng, J., Borsche, M., Liu, Y., and Loew, A.: How representative are instantaneous evaporative fraction measurements of daytime fluxes? *Hydrol. Earth Syst. Sci.*, 17, 3913–3919, 2013.
- Qadir, M., Boers, T.M., Schubert, S., Ghafoor, A., and Murtaza, G.: Agricultural water management in water-starved countries: challenges and opportunities, *Agric. Water Manag.*, 62, 165–85, 2003.
- Raupach, M.: Combination theory and equilibrium evaporation. *Quart. J. R. Met. Soc.*, 127, 1149–1181.
- 30 Ryu, Y., Baldocchi, D. D., Black, T. A., Detto, M., Law, B. E., Leuning, R., Miyata, A., Reichstein, M., Vargas, R., Ammann, C., Beringer, J., Flanagan, L. B., Gu, L., Hutley, L. B., Kim, J., McCaughey, H., Moors, E. J., Rambal, S., and Vesala, T.: On the temporal upscaling of evapotranspiration from instantaneous remote sensing measurements to 8-day mean daily-sums, *Agric. Forest Meteorol.*, 152, 212–222, 2012.



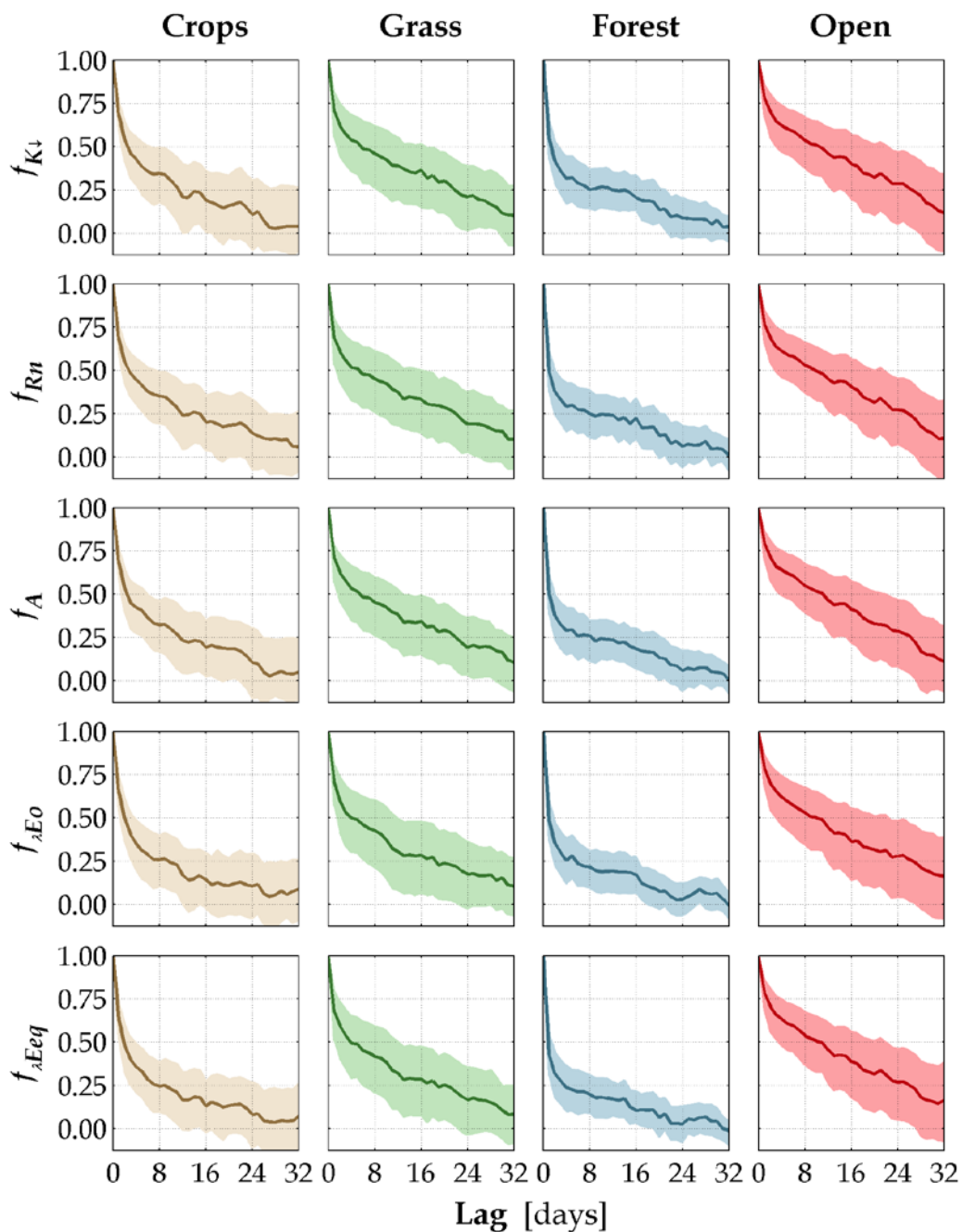
- Seguin, B., and Itier, B.: Using midday surface-temperature to estimate daily evaporation from satellite thermal IR data, *Int. J. Remote Sens.*, 4, 371–383, 1983.
- Schultz, B., and De Wrachien, D.: Irrigation and drainage systems research and development in the 21st century, *Irrig. Drain. Sci.*, 51, 311–327, 2002.
- 5 Suleiman, A., and Crago, R. D.: Hourly and daytime evapotranspiration from grassland using radiometric surface temperatures. *Agron. J.*, 96, 384-390, 2004.
- Tasumi, M., Allen, R. G., Trezza, and Wright, J. L.: 2005. Satellite-based energy balance to assess within-population variance of crop coefficient curves, *J. Irrig. Drain.*, 131, 94-109.
- Thenkabail, P. S., Hanjra, M. A., Dheeravath, V., and Gumma, M.: Global croplands and their water use from remote
10 sensing and nonremote sensing perspectives, in *Advances in environmental remote sensing: sensors, algorithms and applications*, Q. Weng (Ed.), Taylor and Francis, CRC Press, Boca Raton, Florida, USA, 383-420, 2010.
- Trefethen, L. N.: *Approximation theory and approximation practice*. SIAM books, Philadelphia, Pennsylvania, USA, 2013.
- Twine, T. E., Kustas, W. P., Norman, J. M., Cook, D. R., Houser, P.R., Meyer, T. P., Prueger, J. H., Starks, P. J., and
15 Wesely, M. L.: Correcting eddy covariance flux underestimates over a grassland, *Agric. Forest Meteorol.*, 103, 279–300,
2000.
- Van Niel, T. G., McVicar, T. R., Roderick, M. L., van Dijk, A. I. J. M., Renzullo, L. J., and van Gorsel, E.: Correcting for systematic error in satellite-derived latent heat flux due to assumptions in temporal scaling: assessment from flux tower observations. *J. Hydrol.* 409, 140–148, 2011.
- Van Niel, T. G., McVicar, T. R., Roderick, M. L., van Dijk, A. I. J. M., Beringer, J., Hutley, L. B., and van Gorsel, E.:
20 Upscaling latent heat flux for thermal remote sensing studies: Comparison of alternative approaches and correction of bias, *J. Hydrol.*, 468–469, 35–46, 2012.
- Vörösmarty, C. J., McIntyre, P. B., Gessner, M. O., Dudgeon, D., Prusevich, A., Green, P., Glidden, S., Bunn, S. E., Sullivan, C. A., Liermann, C. R., and Davies, P. M.: Global threats to human water security and river biodiversity, *Nature*, 467: 555–561, 2010.
- 25 Wallace, J. S.: Increasing agricultural water use efficiency to meet future food production. *Agric. Ecosyst. Environ.*, 82, 105–19, 2000.
- Wang, K., and Dickinson R. E.: A review of global terrestrial evapotranspiration: Observation, modeling, climatology, and climatic variability, *Rev. Geophys.*, 50, doi: 10.1029/2011RG000373, 2012.
- Willmott, C. J., Ackleson, S. G., Davis, R.E., Feddema, J.J., Klink K.M., Legates, D.R., O'Donnell, J., and Rowe, C.M.:
30 Statistics for the evaluation of model performance. *J. Geophys. Res.*, 90, 8995–9005, 1995.
- Willmott, C., and Matsuura, K.: Advantages of the mean absolute error (MAE) over the root mean square error (RMSE) in assessing average model performance, *Climate Res.*, 30, 79-82, 2005.
- Willmott, C., Robeson, S. M., Matsuura, K., A refined index of model performance, *Int. J. Climitol.*, 32, 2088-2094, 2012.
- Wilks, W. S.: *Statistical Methods in the Atmospheric Sciences*, Academic Press, Burlington, Massachusetts, USA, 2006.



Zhang, L. and Lemeur, R.: Evaluation of daily evapotranspiration estimates from instantaneous measurements, *Agric. Forest Meteorol.*, 74, 139–154, 1995.



Figures



5 Figure 1 The representative autocorrelation function derived for each land cover type and scaled metric used in this study is shown. The shaded area represents one standard deviation about the mean.

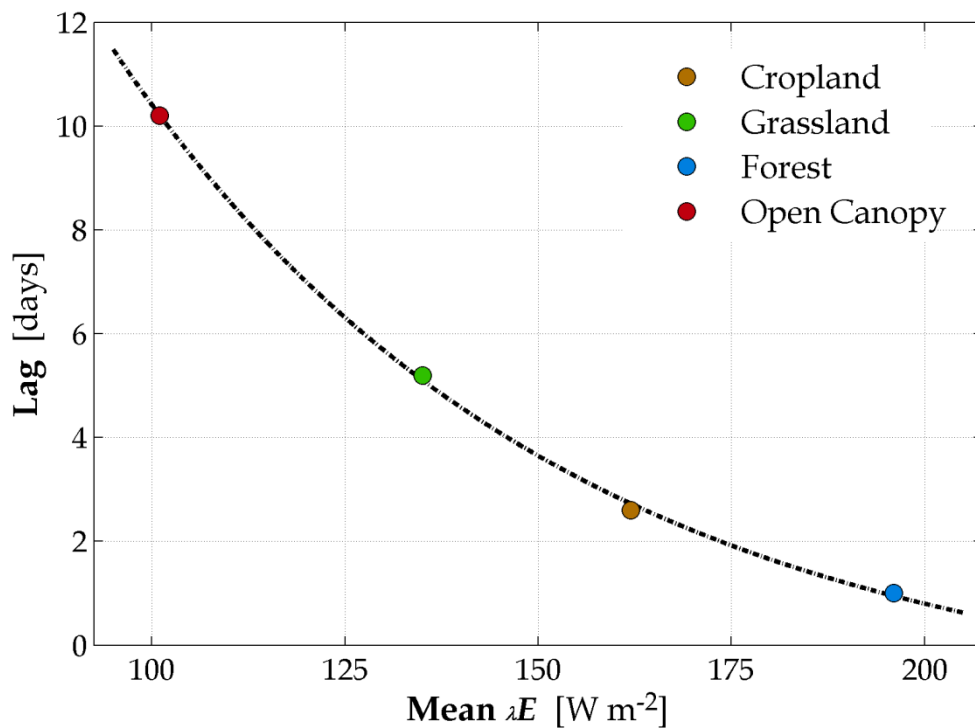


Figure 2 The maximum lag where the autocorrelation function exceeds 0.50 plotted as a function of the mean daytime latent heat flux is shown.

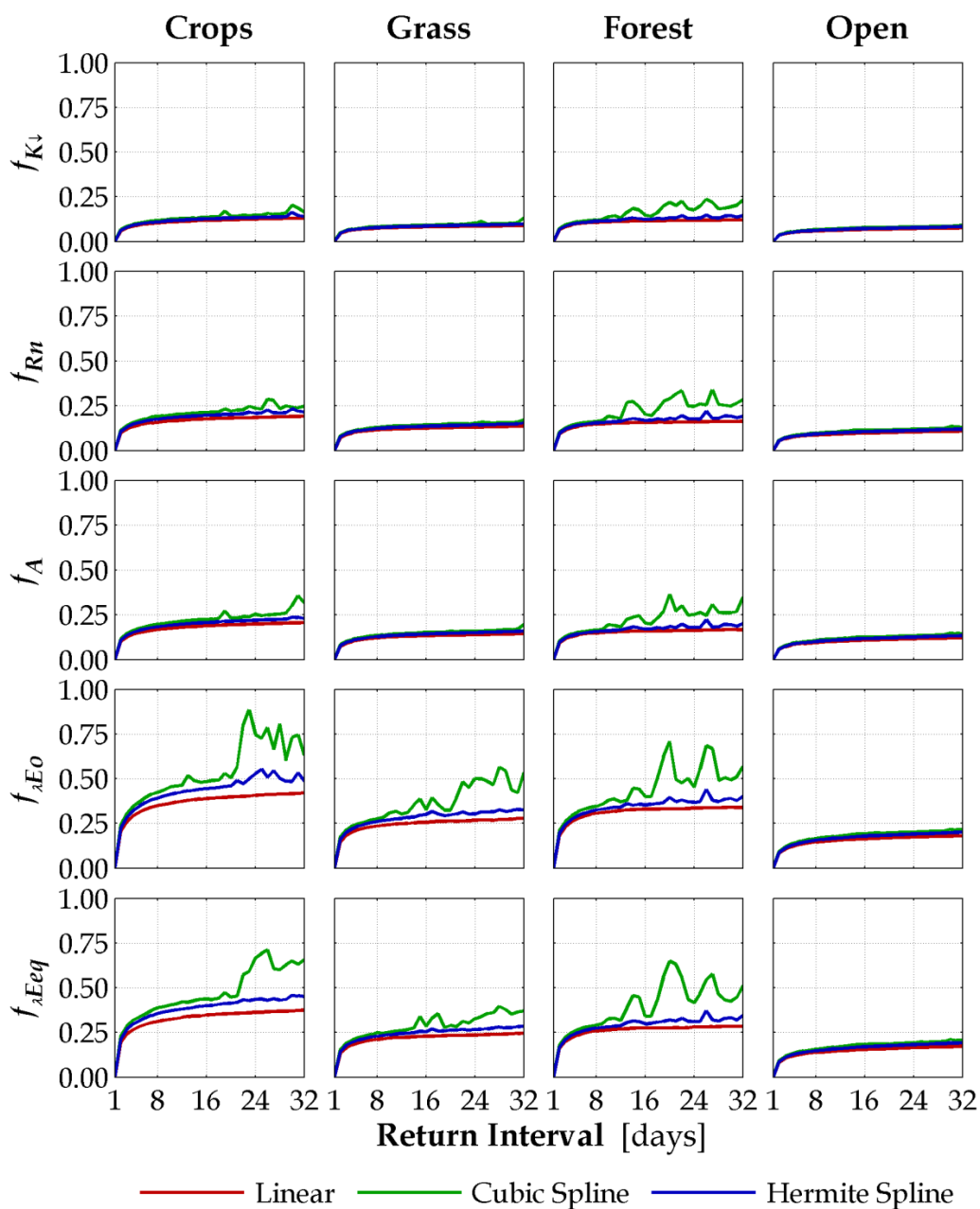


Figure 3 The root mean square error (RMSE) of the estimates of the scaled quantities is shown for each land cover type and interpolation scheme.

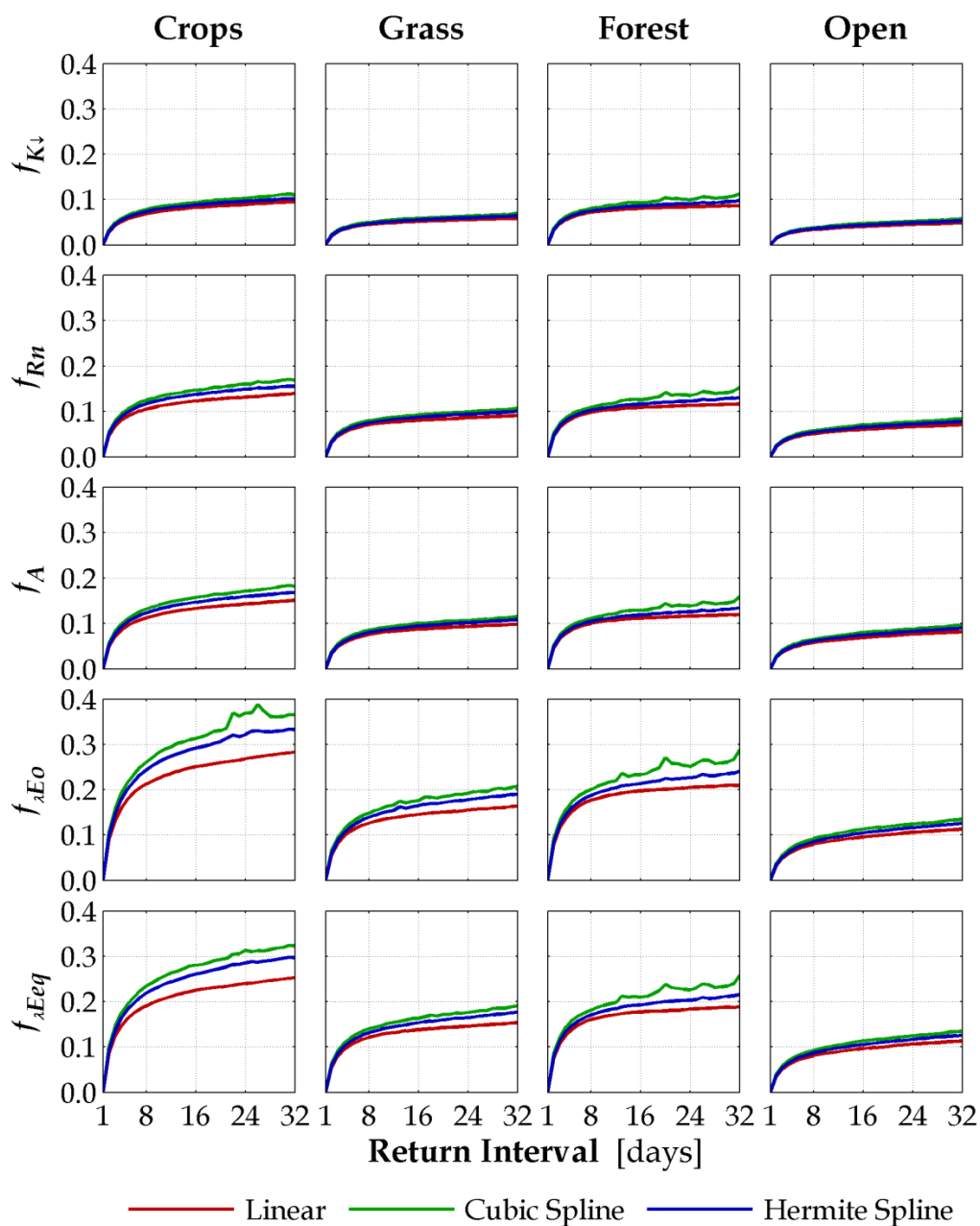


Figure 4 The mean absolute error (MAE) of the estimates of the scaled quantities is shown for each land cover type and interpolation scheme.

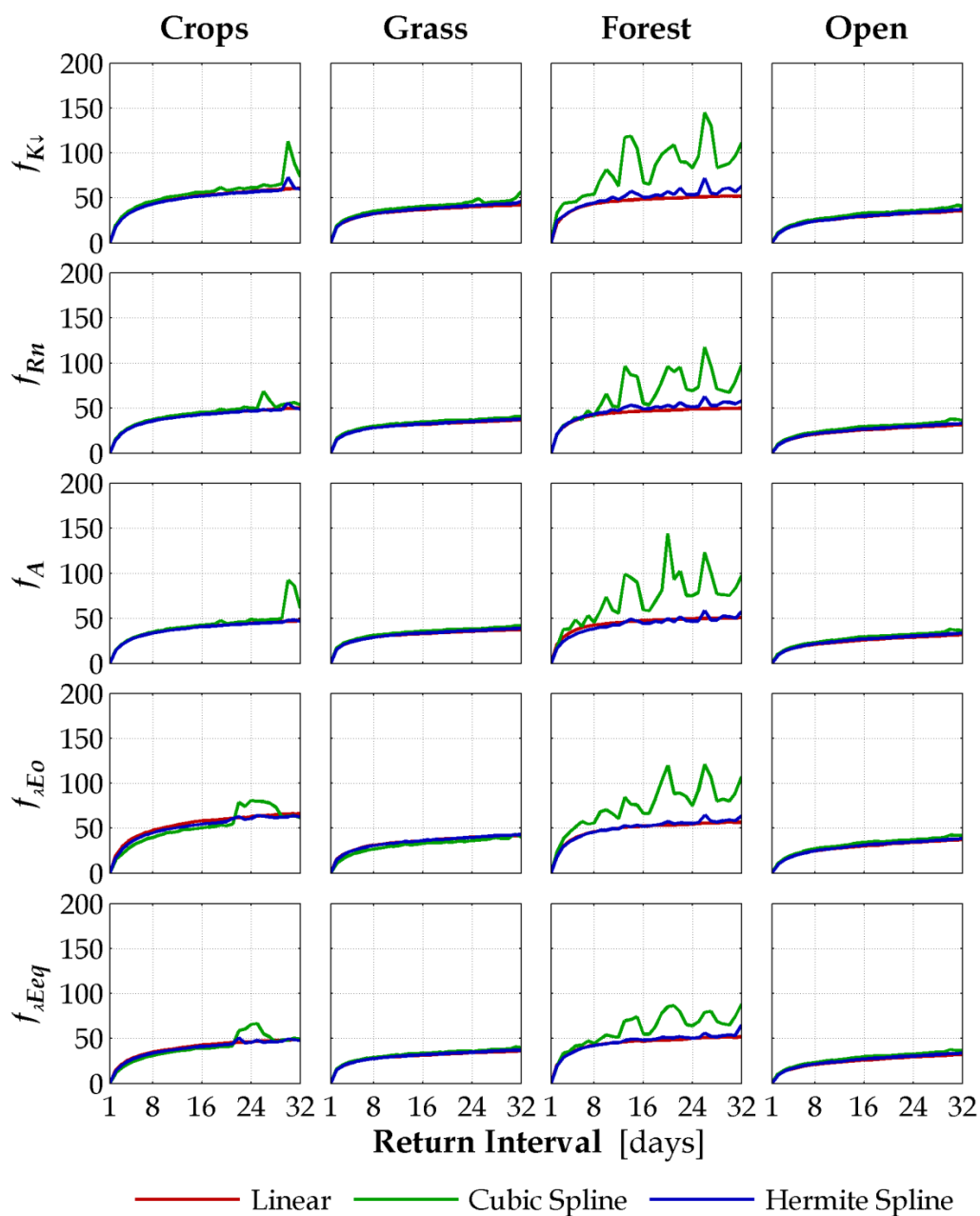


Figure 5 The root mean square error (RMSE) of the latent heat flux derived from each of the scaled quantities is shown for each land cover type and interpolation scheme.

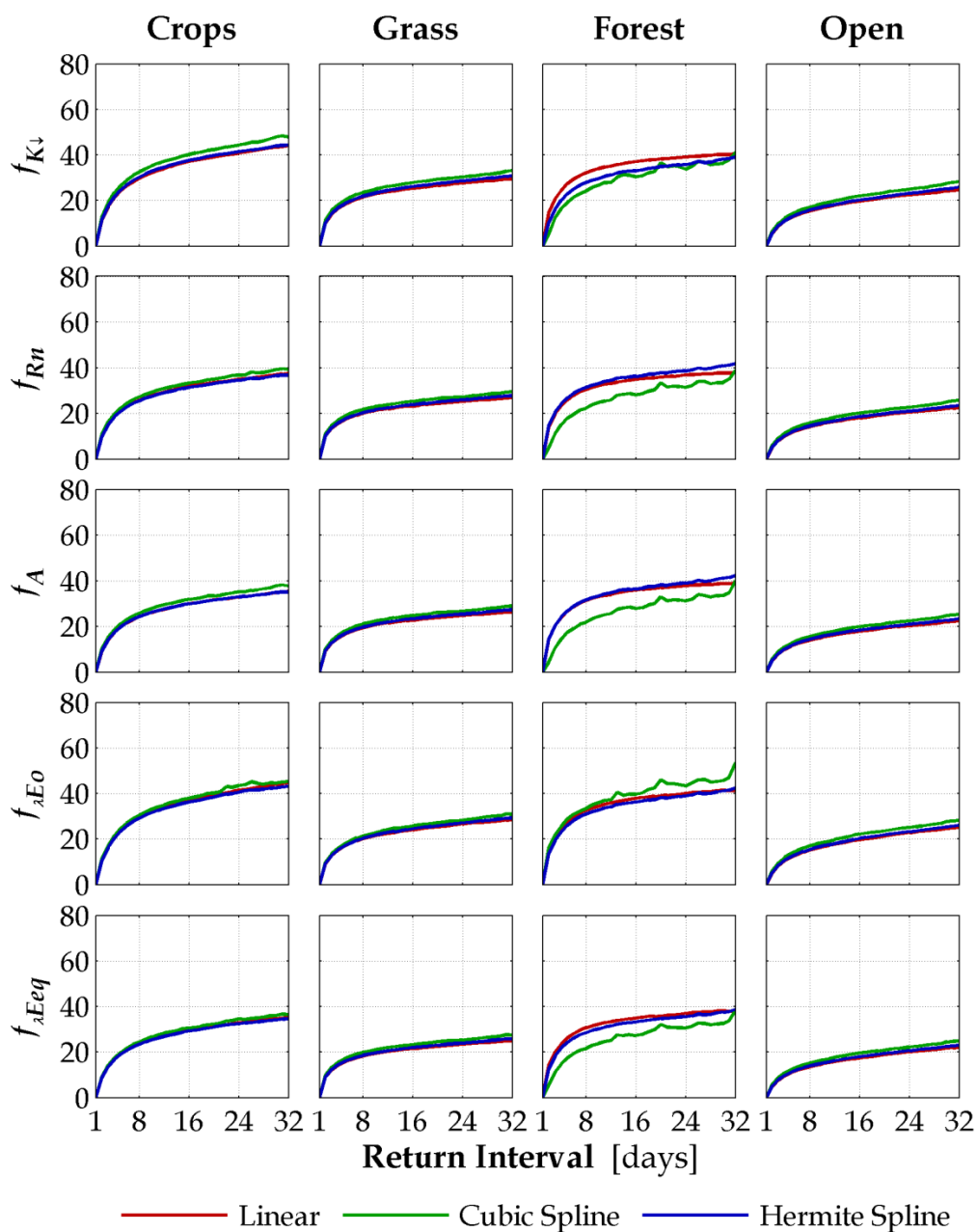


Figure 6 The mean absolute error (MAE) of the latent heat flux derived from each of the scaled quantities is shown for each land cover type and interpolation scheme.

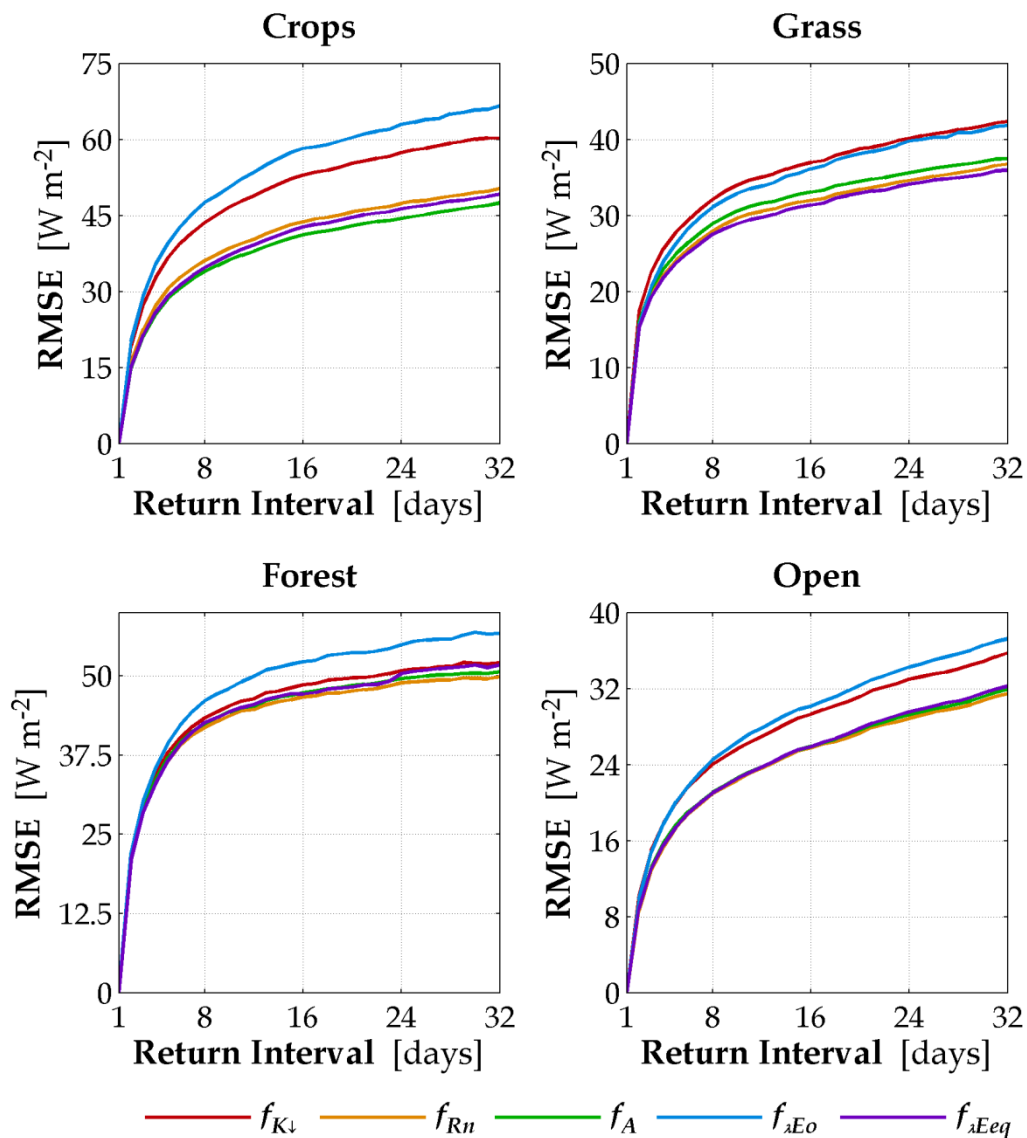


Figure 7 The root mean square error (RMSE) of the latent heat flux derived from each of the scaled quantities is shown for each land cover type when linear interpolation is used.

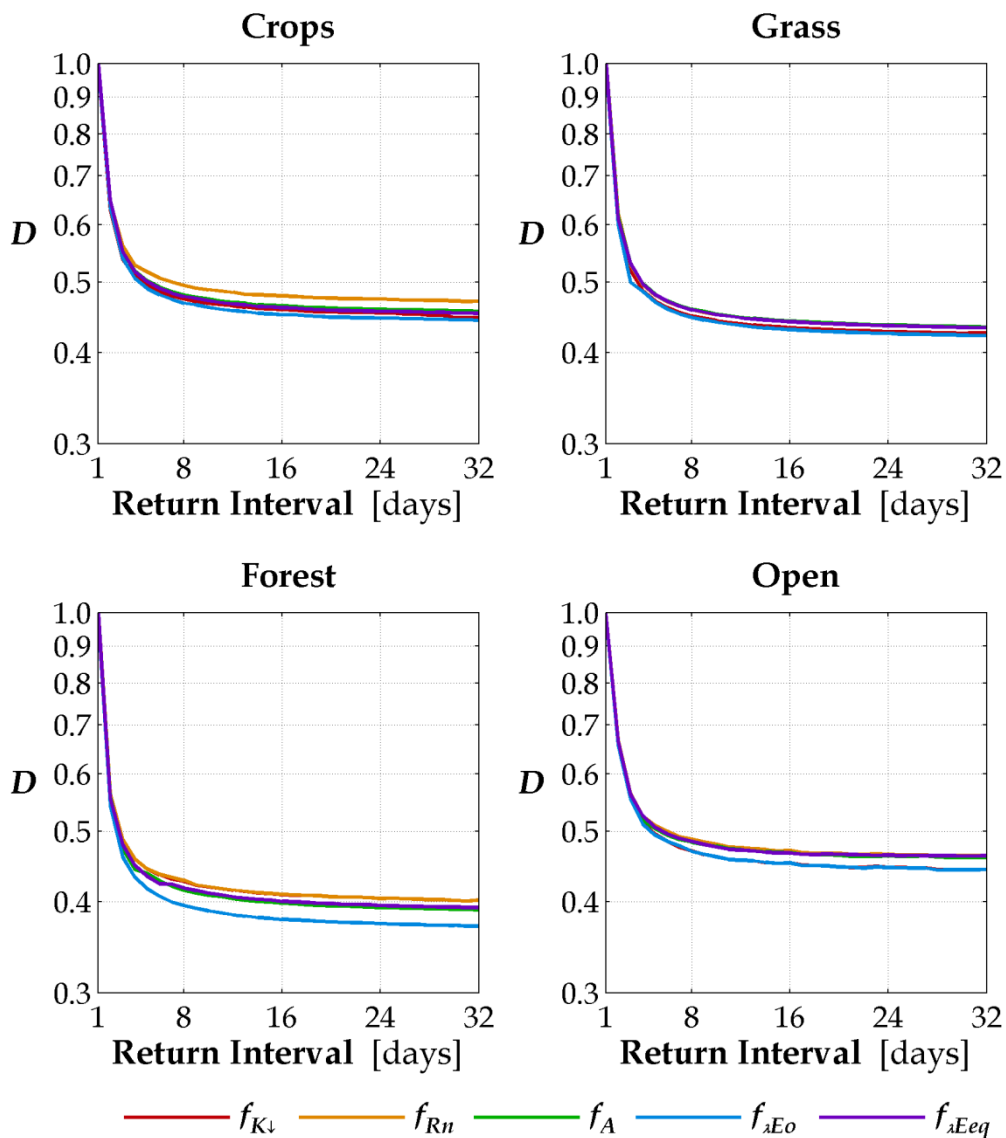


Figure 8 The index of agreement (D) between the observed flux and the latent heat flux derived from each of the scaled quantities is shown for each land cover type when linear interpolation is used.

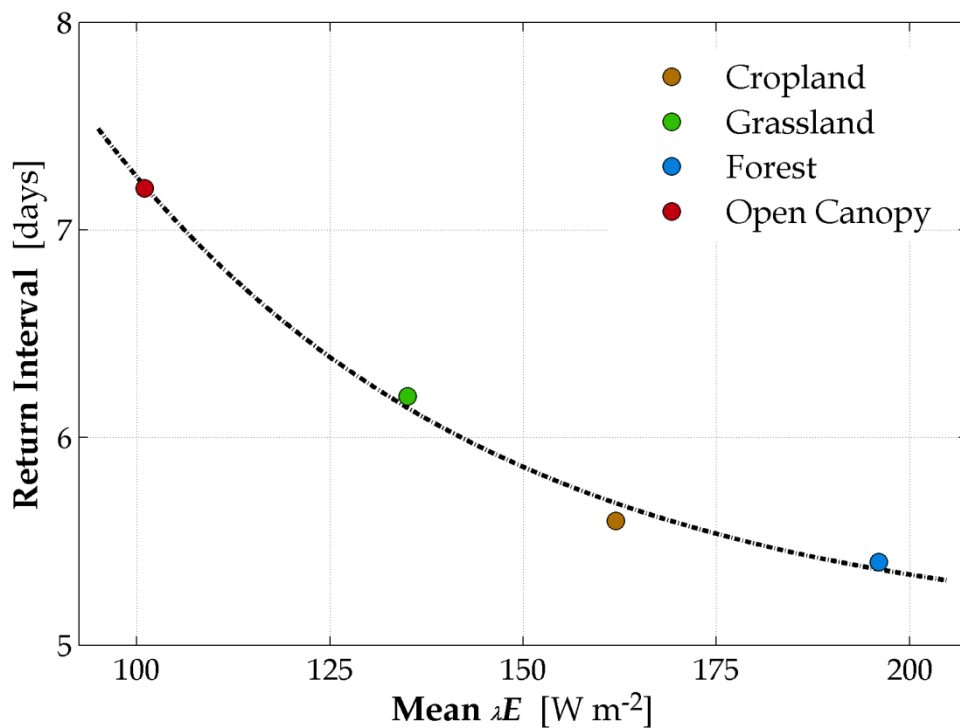


Figure 9 The maximum return interval where the relative error is less than 20% plotted as a function of the mean daytime latent heat flux.



Tables:

Table 1 Summary of the 30-minute measurements collected at each Ameriflux site used in this study.

| Meteorological Conditions | | |
|------------------------------------|---------------------------|-----------------------------|
| Wind Speed | Wind Direction | Air Temperature |
| Water Vapor Density | Vapor Pressure Deficit | Relative Humidity |
| Atmospheric Pressure | Precipitation | |
| Radiation and Energy Budget | | |
| Incident Solar Radiation | Reflected Solar Radiation | Incident Longwave Radiation |
| Terrestrial Longwave Radiation | Net Radiation | Soil Heat Flux |
| Sensible Heat Flux | Latent Heat Flux | Friction Velocity |

**Table 2 Summary of Ameriflux sites used in this study.**

| Site | Location | Land Cover | Site | Location | Land Cover |
|----------------------|-------------------------|-----------------------------------|------------------------|-------------------------|-----------------------------------|
| Bondville | 40.006 °N 88.290 °W | Cropland (maize/soy) | Lucky Hills | 31.744 °N 110.052 °W | Shrubland |
| Brookings | 44.345 °N 96.836 °W | Woody Savanna | Mead | 41.165 °N 96.477 °W | Cropland (maize/soy) |
| Brooks Field | 41.692 °N 93.691 °W | Cropland | Morgan Monroe | 39.323 °N 86.413 °W | Broadleaf Deciduous Forest |
| Chestnut Ridge | 35.931 °N 84.332 °W | Broadleaf Deciduous Forest | Niwot Ridge | 40.033 °N 105.546 °W | Evergreen Needleleaf Forest |
| Fermi Cropland | 41.859 °N 88.223 °W | Cropland (maize/soy) | Missouri Ozarks | 38.744 °N -92.200 °W | Broadleaf Deciduous Forest |
| Fermi Grassland | 41.841 °N 88.241 °W | Grassland | Rosemount | 44.714 °N 93.090 °W | Cropland (maize/soy) |
| Freeman Ranch | 29.940 °N -97.990 °W | Woody Savanna | Santa Rita Mesquite | 31.821 °N 110.866 °W | Woody Savanna |
| Kendall Grassland | 31.737 °N 109.942 °W | Grassland | Tonzi Ranch | 38.432 °N 120.966 °W | Woody Savanna |
| Konza Prairie | 39.082 °N 96.560 °W | Grassland | Vaira Ranch | 38.407 °N 120.910 °W | Grassland |
| Loblolly Pine | 35.978 °N 79.094 °W | Evergreen Needleleaf Forest | Walker Branch | 35.959 °N 84.787 °W | Broadleaf Deciduous Forest |



Table 3 The maximum return interval with a relative error of less than 20% is given for each reference quantity and LULC when linear interpolation was used.

| | | Reference Quantity | | | | |
|-------------------|--------------------|--------------------------|---------------|------------------|----------------------------|------------------------------|
| | | Incident Solar Radiation | Net Radiation | Available Energy | Reference Latent Heat Flux | Equilibrium Latent Heat Flux |
| Land Cover | Cropland | 4 | 6 | 7 | 4 | 7 |
| | Grassland | 5 | 7 | 6 | 5 | 8 |
| | Forest | 5 | 6 | 5 | 5 | 6 |
| | Open Canopy | 6 | 8 | 8 | 7 | 8 |